Neurobiology of Disease 175 (2022) 105932

Contents lists available at ScienceDirect

Neurobiology of Disease

journal homepage: www.elsevier.com/locate/ynbdi

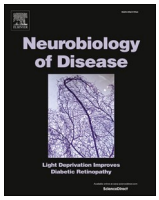

Acute restraint stress impairs histamine type 2 receptor ability to increase the excitability of medium spiny neurons in the nucleus accumbens

Giuseppe Aceto [a,b,1], Luca Nardella [b,1], Giacomo Lazzarino [d], Barbara Tavazzi [d], Alessia Bertozzi [c], Simona Nanni [a,e], Claudia Colussi [a,c], Marcello D'Ascenzo [a,b,2,*], Claudio Grassi [a,b,2]

[a] Fondazione Policlinico Universitario Agostino Gemelli, IRCCS, Largo Agostino Gemelli 8, 00168 Roma, Italy
[b] Department of Neuroscience, Università Cattolica del Sacro Cuore, Largo Francesco Vito 1, 00168 Rome, Italy
[c] Istituto di Analisi dei Sistemi ed Informatica "Antonio Ruberti", National Research Council, Via dei Taurini 19, 00185 Roma, Italy
[d] UniCamillus - Saint Camillus International University of Health and Medical Sciences, Via di Sant'Alessandro 8, 00131 Rome, Italy
[e] Department of Translational Medicine and Surgery, Università Cattolica del Sacro Cuore, Largo Francesco Vito 1, 00168 Rome, Italy

ARTICLE INFO

Keywords:
Acute restraint stress
Histamine
H2 receptor
Kv4.2
Nucleus accumbens
Intrinsic excitability

ABSTRACT

Histamine, a monoamine implicated in stress-related arousal states, is synthesized in neurons exclusively located in the hypothalamic tuberomammillary nucleus (TMN) from where they diffusely innervate striatal and mesolimbic networks including the nucleus accumbens (NAc), a vital node in the limbic loop. Since histamine-containing TMN neuron output increases during stress, we hypothesized that exposure of mice to acute restrain stress (ARS) recruits endogenous histamine type 2 receptor (H2R) signaling in the NAc, whose activation increases medium spiny neurons (MSNs) intrinsic excitability via downregulation of A-type K^+ currents. We employed an ARS paradigm in which mice were restrained for 120 min, followed by a 20-min recovery period, after which brain slices were prepared for ex vivo electrophysiology. Using whole-cell patch-clamp recordings, we found that pharmacological activation of H2R failed to affect MSN excitability and A-type K^+ currents in mice that underwent ARS. Interestingly, in mice treated with H2R-antagonist prior to ARS paradigm, H2R activation increased evoked firing and decreased A-type K^+ currents similarly to what observed in control mice. Furthermore, H2R-antagonist treatment ameliorated anxiety-like behavior in ARS mice. Together, our findings indicate that ARS paradigm recruits endogenous H2R signaling in MSNs and suggest the involvement of H2R signaling in stress-related motivational states.

1. Introduction

Although appropriate responses to stress are essential for an individual's adaptation and survival, stressful events are considered a primary risk factor for most neuropsychiatric disorders including anxiety, depression, and post-traumatic stress disorder (PTSD) (Duman et al., 2016; McEwen et al., 2015; Pitman et al., 2012). Despite the underling causative molecular mechanisms of stress-related disorders are still poorly understood, strong evidence indicates that brain region-specific changes in signaling pathways, neuroplasticity, neuroinflammation, are primarily involved. Specifically, alterations in the nucleus accumbens (NAc) circuitry, part of the reward circuit, are thought to play a key role in stress-related disorders (Francis and Lobo, 2017). The NAc receives dense glutamatergic innervation from the prefrontal cortex (PFC), amygdala, and hippocampus in addition to dopaminergic modulation from the ventral tegmental area (VTA). It serves as a central integration point of motor, limbic, and cognitive information and may act as a hub between stress and reward-responses, resulting in affective action selection (Nestler and Carlezon Jr., 2006).

One of the neurotransmitters that is profoundly affected by stress is

* Corresponding author at: Department of Neuroscience, Università Cattolica del Sacro Cuore, Largo Francesco Vito 1, 00168 Rome, Italy.
E-mail addresses: giuseppe.aceto1@unicatt.it (G. Aceto), luca.nardella@unicatt.it (L. Nardella), giacomo.lazzarino@unicamillus.org (G. Lazzarino), barbara.Tavazzi@unicatt.it (B. Tavazzi), alessia.bertozzi@iasi.cnr.it (A. Bertozzi), simona.nanni@unicatt.it (S. Nanni), claudia.colussi@cnr.it (C. Colussi), marcello.dascenzo@unicatt.it (M. D'Ascenzo), claudio.grassi@unicatt.it (C. Grassi).
[1] These authors contributed equally to this work.
[2] These authors shared senior authorship

https://doi.org/10.1016/j.nbd.2022.105932
Received 31 August 2022; Received in revised form 7 November 2022; Accepted 21 November 2022
Available online 23 November 2022

histamine which is classically associated to different physiological functions, such as the sleep–wake cycle, sensory and motor functions, energy and endocrine homeostasis, cognition and attention (Arrigoni and Fuller, 2021; Nomura et al., 2019; Panula and Nuutinen, 2013; Provensi et al., 2020; Venner et al., 2019; Yoshikawa et al., 2021). Early experimental evidence has shown that histaminergic neurons, exclusively located in the hypothalamic tuberomammillary nucleus (TMN), significantly increase their activity in rats exposed to acute stress (Mazurkiewicz-Kwilecki and Prell, 1986). In addition, it was found that acute stress increased the histamine levels in rat nucleus accumbens (NAc), cerebral cortex and diencephalon (Ito, 2000; Taylor and Snyder, 1971). More recently, it has been reported that stress-evoked histamine signaling recruits a presynaptic gain control mechanism at glutamatergic synapses in the NAc (Manz et al., 2021). Moreover, the activation of the histaminergic afferent system inhibits glutamatergic synaptic transmission in the circuit from the prelimbic prefrontal cortex to the NAc and improves anxiety-like behavior induced by restraint stress (Zhang et al., 2020).

In the context of the neuronal signaling pathways activated by histamine receptors, we recently showed that histaminergic transmission in the NAc increases medium spiny neurons (MSNs) intrinsic excitability through histamine type 2 receptor (H2R), the prevailing postsynaptic histamine receptor expressed in NAc MSNs (Aceto et al., 2022). In particular, this study showed that pharmacological activation of these receptors strongly increases the evoked-firing through a mechanism that requires protein kinase A (PKA) signaling and downregulation of Kv4.2-mediated currents (Aceto et al., 2022). Building on this evidence and considering that histamine-containing TMN neuron output is increased during acute stress (Ito, 2000; Manz et al., 2021), we posited that alterations of intrinsic excitability induced by H2R signaling could be a causative link and a converging mechanism underlying anxiety-like behaviors in stress animal models. To test this hypothesis we studied the role of H2R-dependent modulation of evoked firing in NAc MSNs of mice exposed to acute restraint stress (ARS), a well-established animal model of stress-associated behavioral states (Buynitsky and Mostofsky, 2009; Zhang et al., 2020).

2. Materials and methods

2.1. Animal and ethical approval

Male C57BL/6 J mice, bred in house, were maintained on a 12-h light/dark cycle, in a temperature and humidity-controlled room with ad libitum access to mouse chow and water. Four/five-week-old mice were used. All animals procedures were approved by the Ethics Committee of the Catholic University and complied with Italian Ministry of Health guidelines, national laws (Legislative Decree 116/1992; Ethics approval number: n° 766/2021-PR) and European Union guidelines on animal research (No. 86/ 609/EEC).

2.2. Acute restraint stress (ARS)

The ARS model was adapted from previous procedures. Four/five weeks old mice were subjected to ARS for 2 h using polycarbonate cylinders (20 cm long, 6.5 cm in diameter)(Sadler and Bailey, 2016). The mice could not move freely or turn around but were not oversqueezed; this procedure induces chronic stress but not pain or injury. Mice were distributed in the control group or the stress group. Stress group mice were removed from the restrainers and allowed to move freely in their home cages 30 min before the behavioral tests in order to avoid non-specific motor effects due to movement restriction. Mice in the control group were left in their usual environment and were undisturbed. In a subset of experiments Zolantidine dimaleate (an H2 receptor antagonist; Tocris Bioscience, Bristol, UK) was injected intraperitoneally (ip) at a final dose of 10 mg/kg.

2.3. Behavioral assessment

Anxiety responses were measured in the EPM test. The procedure was similar to the method previously developed and validated from (Lister, 1987). The maze consisted of two opposing open arms (30 × 5 cm) and two equal-sized closed (30 × 5 × 15 cm) arms opposite each other, made of Plexiglas and elevated at a height of 50 cm from the floor. Each testing session began by placing the mouse on the central platform of the maze (5 × 5 cm) facing an open arm. The subject was allowed 5 min of free exploration. The parameters measured were time spent in the open arm and time spent in the closed arm. Between animals, the maze was thoroughly cleaned with dilute 70% alcohol and dry cloths before each session to get rid of residual odor. All tests were conducted under moderate illumination during the light phase of the diurnal cycle.

2.4. Slice preparation and electrophysiology

Coronal slices (300 μm) containing the nucleus accumbens were prepared as previously described (Aceto et al., 2022; D'Ascenzo et al., 2009). C57/BL/6 J mice (P28–40) were anesthetized with isoflurane and euthanized by cervical dislocation and decapitated. The brains were rapidly removed and placed in ice-cold, sucrose-based cutting solution containing the following (in mM): TRIS-HCl 72, TRIZMA base 18, NaH2PO4 1.2, $NaHCO_3$ 30, KCl 2.5, glucose 25, HEPES 20, MgSO4 10, Na-pyruvate 3, ascorbic acid 5, $CaCl_2$ 0.5, sucrose 20. NAc slices (300 μm thick) were cut on a vibratome (VT1200S; Leica Microsystems, Germany) and immediately transferred to an incubation chamber held at 32 °C and filled with a recovery solution containing (in mM): TRIS-HCl 72, TRIZMA base 18, NaH_2PO_4 1.2, $NaHCO_3$ 25, KCl 2.5, glucose 25, HEPES 20, $MgSO_4$ 10, Na-pyruvate 3, ascorbic acid 5, $CaCl_2$ 0.5, sucrose 20. After 30 min, slices were transferred to a second incubation chamber held at 32 °C and filled with artificial cerebrospinal fluid (aCSF) containing the following (in mM): NaCl 124, KCl 3.2, NaH_2PO_4 1.2, $MgCl_2$ 1, $CaCl_2$ 2, $NaHCO_3$ 26, and glucose 10, pH 7.4. During incubations, the chambers were continuously bubbled with 95% O_2/5% CO_2. Finally, slices were equilibrated at RT for at least 30 min. For electrophysiological recordings, slices were transferred to a submerged recording chamber constantly perfused with heated aCSF (32 °C) and bubbled with 95% O_2/5% CO_2. MSNs of the NAc were visualized under DIC infrared illumination. Patch pipettes had a resistance of 4–6 MΩ when filled with an internal solution containing (in mM): K-gluconate 145, $MgCl_2$ 2, HEPES 10, EGTA 0.1, Na-ATP 2.5, Na-GTP 0.25, phosphocreatine 5, pH adjusted to 7.2 with KOH.

Recordings were performed using a Multiclamp 700B/Digidata 1550A system (Molecular Devices, USA) and digitized at a 10,000 Hz sampling frequency. All the electrophysiological recordings were analyzed using the Clampfit 10.9 software (Molecular Devices). Evoked firings were recorded in whole-cell, current-clamp mode. Only cells with a stable resting membrane potential negative to −80 mV, overshooting action potentials (exceeding 75–80 mV threshold-to-peak) and an input resistance >100 MΩ were included. Furthermore, cells were rejected if resting membrane potential and input resistance changed >20%. The membrane input resistance was measured by a series of 600 ms hyperpolarizing current steps from −50 to 0 pA, step 10 pA with 1 s interval.

To test the firing properties of MSNs in the NAc core and shell subregions during continuous depolarization, we exposed these cells to a somatic current pulse a series of 1 s of somatic current pulses (every 5 s). Currents levels were chosen based on minimum amplitudes required to elicit a stable firing of 4–8 action potentials. Beginning with 80 pA, the injected current was gradually increased in 10–50 pA increments until these criteria were satisfied. Of note, during interpulse intervals, membrane potentials where kept to the resting value (~80 mV) by injecting hyperpolarizing/depolarizing currents to counteract possible H2R-dependent depolarization (Zhuang et al., 2018). Local exposure of the recorded MSN to 10 μM dimaprit (for 1 min) was achieved by placing a glass pipette (~5 μm tip diameter) 40–100 μm away from the cell body

with continuous pressure of ~0.5–1 psi. All the electrophysiological parameters were analyzed 10–30 s (pre) and 1–2 min (post) drugs application.

Action potential threshold values were calculated from waveform averages by determining the first point of sustained positive acceleration (second derivative) of voltage that exceeded 2 SDs of the acceleration "noise" 5–10 ms prior to threshold. Measurements of action potential half-width and all action potential properties were taken from waveform averages representing 1 s per condition. AHP voltages were measured individually from raw traces prior to averaging.

The transient A-type K^+ current in voltage–clamp mode was recorded applying 400 ms voltage step from −110 to +40 mV. Prepulse of hyperpolarization at −110 mV for 100 ms removed A-type K^+ channel inactivation and enabled subsequent maximum activation. The transient channel was inactivated by the same voltage steps that preceded a depolarizing pre-pulse of −10 mV for 100 ms, leaving the sustained current of the total outward current. The transient current was then isolated by a digital subtraction of the sustained current from the total outward current. To record A-type K^+ current the following reagents were added to the external solution: 1 μM tetrodotoxin (TTX); 300 μM Cd^{2+} and 20 mM of tetraethylammonium (TEA). Excitatory and inhibitory synaptic transmission were also blocked using NBQX (10 μM) and picrotoxin (50 μM). Membrane capacitances and series resistences (Rs) were compensated electronically. Rs before compensation were in the range of 5–20 MΩ and were routinely corrected by 75–85%. Data obtained from a given cell were rejected if Rs were larger than 20 MΩ or changed by >20% during the course of the experiment.

Analysis and curve fitting were conducted in Clampfit 10.9 (Molecular Devices) and SigmaPlot 14.0 (Systat Software Inc. San Jose, CA). The peak conductance (Gp) was calculated as Gp = Ip/(Vc − Vrev), where Ip is the peak outward current, Vc is the command voltage and Vrev is the estimated reversal potential for K^+ (−95 mV). The Gp–V relations were described assuming a first-order Boltzmann function: Gp (V) = Gpmax1/ (1 + exp. ((Vc − $V_{1/2a}$)/ka), where Gpmax is the maximal peak conductance, ka is the slope factor and $V_{1/2a}$ is the activation midpoint voltage.

2.5. Western blot assay

Western blot experiments were performed as previously described (Aceto et al., 2022). Briefly, tissues were lysed in ice-cold lysis buffer (NaCl 150 mM,Tris-HCl 50 mM pH 7.4, EDTA 2 mM) containing 1% Triton X-100, 0.1% SDS, 1 × protease inhibitor cocktail (Sigma-Aldrich, St Louis, MO, USA), 1 mM sodiumorthovanadate (Sigma-Aldrich) and 1 mM sodiumfluoride (Sigma-Aldrich). Lysates were incubated for 10 min on ice with occasional vortexing and spun down at 22000 *g* at 4 °C. The supernatant was quantified for protein content (DC Protein Assay; Bio-Rad, Hercules, CA, USA). Equal amounts of protein were diluted in Laemmli buffer, boiled and resolved by SDS-PAGE. Primary antibodies for anti-Kv4.2 (WB 1:1000, monoclonal, Neuromab 75–016), anti-H2R (WB 1:1000, polyclonal, Abcam, 108,540), anti-tubulin (WB 1:2000, polyclonal, Abcam ab8227; Cambridge, MA, USA) were incubated overnight and revealed with HRP-conjugated secondary antibodies (Cell Signaling Technology). Expression was evaluated and documented by using UVItec Cambridge Alliance. The band of interest was normalized to the housekeepeing (Tubulin) and expressed as fold change versus control. Images shown were cropped for presentation with no manipulations.

2.6. Cellular fractioning

Brain slices were suspended in Syn-PER reagent (Thermo Fisher, Waltham, MA, USA) containing protease and phosphatase inhibitors (Sigma-Aldrich) to specifically separate membranes from cytosol. Tissues were gently homogenized in a pre-chilled Dounce tissue grinder with 15 slow strokes and the lysate was centrifuged at 1200 *g* for 10 min at 4 °C. The pellet was discarded and the supernatant centrifuged at 15000 *g* for 20 min at 4 °C. The supernatant, containing the cytosolic fraction, was saved for western blotting analysis and the pellet, containing the membrane fractions, was resuspended in RIPA buffer plus 0.1% SDS and vortexed for 15 s every 10 min for a total of 40 min to dissolve the proteins. Extracts were quantified (Bio-Rad) and analyzed by western blotting.

2.7. Histamine determination by high performance liquid chromatography

Brains were microdissected to obtain nucleus accumbens regions and tissues were stored in liquid nitrogen until processing for the HPLC determination of histamine. Tissue was performed using the organic solvent deproteinizing procedure described in detail elsewhere with some slight modifications (Lazzarino et al., 2020). Briefly, 500 μl of ice-cold precipitating solution, composed of 75% HPLC grade CH_3CN + 25% 10 mM KH_2PO4 pH 7.40, were added to the frozen tissues, collected from restraint and control mice. An Ultra-Turrax homogenizer set at 24,000 rpm/min (Janke & Kunkel, Staufen, Germany) allowed to obtain the preparation of a fine homogenate in 90 s. Tissue homogenates were then centrifuged at 20,690 ×*g* for 10 min at 4 °C, the obtained pellets were utilized for the total amount of protein determination and the clear supernatants were saved and subjected to two HPLC-grade $CHCl_3$ washings to eliminate the organic solvent and obtain an upper aqueous phase that was directly injected onto the HPLC.

A Surveyor HPLC system (ThermoFisher Italia, Rodano, Milan, Italy) equipped with a highly-sensitive photodiode array detector provided with a 5 cm light path flow cell, and set up between 200 and 400 nm wavelength, was used for the sample analyses. Data acquisition and analyses were performed using the ChromQuest® software package provided by the HPLC manufacturer. Histamine and the internal standard norvaline, were automatically derivatized before injection with a mixture of 25 mmol/l orthophtalaldehyde (OPA), 1% of 3-methylpropionic acid (MPA) and 237.5 mmol/l sodium borate, pH 9.8, as described in detail elsewhere with some slight modifications in the chromatographic conditions (Amorini et al., 2017). The automated precolumn derivatization of the samples with OPA-MPA was carried out at 25 °C and 50 μl of the derivatized mixture were loaded onto a Hypersil C-18, 250 × 4.6 mm, 5 μm particle size HPLC column, thermostated at 21 °C during chromatographic runs. The flow rate was 1.2 ml/min and a step gradient with two mobile phases (A = 24 mmol/l CH_3COONa + 24 mmol/l Na_2HPO_4 + 1% tetrahydrofurane +0.1% trifluoroacetic acid, pH 8; B = 40% CH_3OH + 30% CH_3CN + 30% H_2O), allowed the separation and quantification of histamine. Assignment and calculation of the OPA-histamine in chromatographic runs were carried out at 338 nm wavelengths by comparing retention time and area of the peak with that of chromatographic runs of freshly prepared ultra-pure true histamine solutions with known concentrations. In the NAc tissue extracts, the total amount of proteins was determined according to the Bradford method (Bradford, 1976). Histamine concentrations in tissue extracts were normalized for the total tissue protein concentrations and expressed as nmol/mg of proteins.

2.8. Statistical analysis

Throughout this study, data are shown as means ± standard error of the means (SEM) and the number of cells (n) and mice are indicated. Data in the figures are plotted showing both single cells and averaged data. Statistical significance was assessed with either Student's *t*-test or one-way ANOVA for multiple-group comparisons (with the Bonferroni post hoc test). Statistical analysis was performed with the SYSTAT 10.2 software (Systat Software, Chicago, IL, USA). Two-tailed, non-parametric statistical comparisons were performed using the Wilcoxon signed-rank (WSR) test for paired data or the Mann–Whitney U (MWU) test for unpaired data. The level of significance was set at 0.05.

3. Results

3.1. Pharmacological activation of H2R fails to increase MSN excitability in the NAc of mice exposed to acute restraint stress

Experimental evidence indicates that histamine-containing TMN neuron output increases during acute stress (Ito, 2000; Manz et al., 2021; Miklos and Kovacs, 2003). Thus, we asked whether ARS recruits endogenous H2R signaling pathway in NAc MSNs. We employed a restraint paradigm in which mice were restrained for 120 min (see methods), followed by a 20-min recovery period, after which brain slices were prepared for ex vivo electrophysiology (Fig. 1A). We hypothesized that ARS engages TMN-to-NAc volume transmission, thereby altering the capability of H2R activation to affect evoked firing in MSNs.

To determine the effects of H2R activation on MSN excitability in the NAc core and shell, we performed whole-cell patch-clamp recordings of visually identified MSNs (see methods) in brain slices during local perfusion of dimaprit (10 μM), a selective agonist of H2R. The firing properties of MSNs were studied by applying 1-s somatic current pulses, whose levels were chosen, in each recorded MSN, to elicit a stable firing of 4–8 action potentials.

In accordance with results collected in our previous study, in control mice local perfusion of dimaprit robustly increased the number of action potentials (AP) during somatic current pulses (Fig. 1B and C; number of APs: pre = 4.28 ± 0.38; post = 9.27 ± 1.33; $n = 12$ cells from 4 mice; $p = 0.0003$; paired Student's t-test). However, in mice that underwent ARS protocol, dimaprit perfusion failed to significantly affect neuronal firing (Fig. 1 *E* and *F*; number of APs: pre = 6.26 ± 0.60; post = 6.51 ± 0.86; $n = 12$ from 4 mice; $p = 0.573$; paired Student's t-test).

MSNs of the NAc are typically classified as dopamine D1 and D2 receptor subtypes, which belong to the direct and indirect pathway (Kupchik et al., 2015). To evaluate whether H2R is expressed in both NAc MSN subpopulations we assessed H2R, D1R and D2R mRNA levels using a protocol that combines whole-cell patch-clamp recordings with high-quality single cell RNA analysis by ddPCR (single-cell qRT-ddPCR) (Cadwell et al., 2016; Possieri et al., 2021). As shown in Supplementary

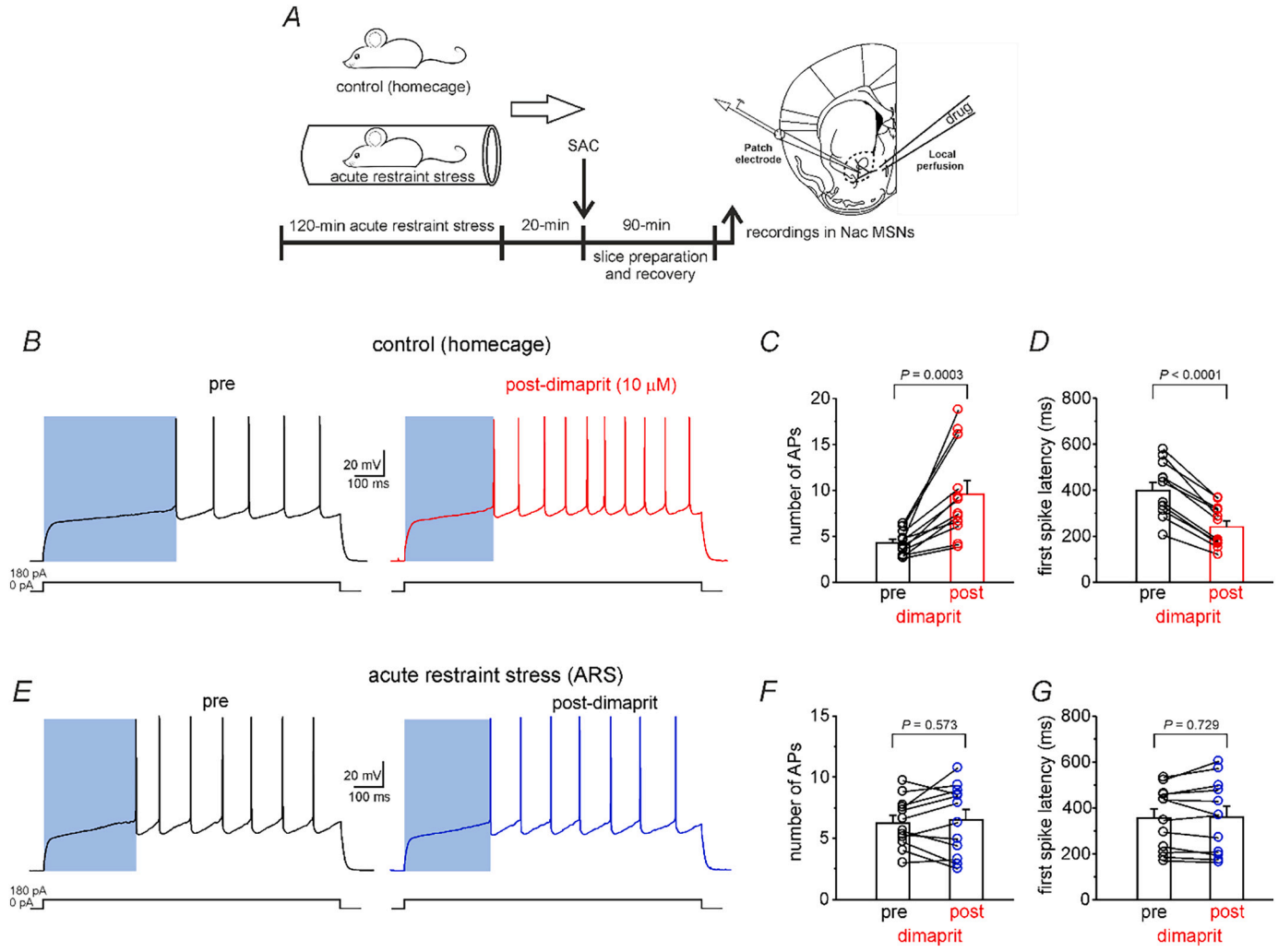

Fig. 1. Pharmacological activation of H2R does not enhance the frequency of evoked firing in MSNs of mice exposed to acute restraint stress. (A) Left, schematic depicting 120-min ARS paradigm and recording strategy in MSNs of control and restraint mice. On the right schematic diagram of a brain section at NAc level with the patch pipette located in the MSN soma and the local perfusion system located 50–100 μm away from the recording electrode. (*B*) Representative traces showing current-evoked firing of a MSN before (black) and after 1 min (red) local perfusion of H2R agonist (dimaprit; 10 μM) in control mice. The current-evoked firing protocol is depicted on the bottom. (*C*) Bar graph depicting quantification of evoked firing in the experimental conditions showed in panel B. Bars represent normalized mean ± SEM ($n = 12$ cells from 4 mice; $p = 0.0003$; paired Student's t-test;). (*D*) Summary plot showing reduced first spike latency following dimaprit perfusion ($n = 12$ cells from *4* mice; $P < 0.0001$; paired Student's t-test). (*E*) Representative traces and summary plot (*F and G*) illustrating that the evoked firing and first spike latency were not affected by dimaprit application in mice exposed to ARS protocol (evoked firing: $n = 12$ cells from = 4 mice; $p = 0.573$; paired Student's t-test; first spike latency: $n = 12$ cells from 4 mice; $p = 0.729$; paired Student's t-test). SAC, sacrifice. (For interpretation of the references to colour in this figure legend, the reader is referred to the web version of this article.)

Fig. 1, mRNA levels of H2R were comparable in single MSNs expressing D1R or D2R MSNs suggesting that H2R signaling pathway increases evoked firing in both types of MSNs.

In naive mice, enhanced MSN excitability after H2R activation was associated with: i) decreased latency to fire, ii) decreased action potential afterhyperpolarization (AHP), and iii) increased action potential half-width (Aceto et al., 2022).

Therefore, we measured medium AHP (mAHP) peak voltages before and after dimaprit application in control and ARS exposed mice. As shown in Fig. 1D, first spike latency was significantly reduced in control mice (first spike latency: pre = 398.7 ± 35.0 ms; post = 240.2 ± 26.6 ms; $n = 12$ cells from 4 mice; $P < 0.0001$; paired Student's t-test) but not in ARS mice (Fig. 1G; first spike latency: pre = 356.2 ± 40.5 ms; post = 360.2 ± 47.7 ms; $n = 12$ cells from 4 mice; $p = 0.729$; paired Student's t-test). Moreover, as shown in Fig. 2, we observed a significant reduction in mAHP after dimaprit application in control mice (Fig. 2A; mAHP amplitude: pre = 9.41 ± 0.52 mV; post: 7.8 ± 0.54 mV; $n = 12$ cells from 4 mice; $p = 0.0008$; paired Student's t-test), an effect that was not detected in mice underwent ARS (Fig. 2C; mAHP amplitude: pre = 9.03 ± 0.76 mV; post: 9.0 ± 8.7 mV; $n = 17$ cells from 4 mice, $p = 0.919$; paired Student's t-test). Consistently, the significant increase of the AP half-width observed in control mice was not found in ARS mice (Fig. 2B; control mice: AP half-width: pre = 1.15 ± 0.09 ms; post = 1.27 ± 0.11 ms; n = 12 cells from 4 mice; $p = 0.0039$; paired Student's t-test; Fig. 2D; ARS mice: AP half-width: pre = 1.33 ± 0.1 ms; post = 1.29 ± 0.09 ms; n = 12 cells from 4 mice; $p = 0.125$; paired Student's t-test).

These results suggest that stress-induced histamine release in the NAc occludes subsequent dimaprit-dependent increased evoked firing likely because of saturation of the H2R signaling pathway. To corroborate these findings we performed a new set of experiments and compared the levels of histamine in the NAc tissues from control and ARS mice by using high sensitive HPLC method as previously described (Amorini et al., 2017). In line with previous studies, ARS significantly increased the NAc histamine levels compared to those measured in the control group (Supplementary Fig. 2A; 480 ± 60 nmoli/mg protein versus 223 ± 22 nmoli/mg protein; $n = 6$ for both groups; unpaired t-test; $p = 0.0013$). Moreover, to rule out the possibility that the absence of dimaprit's effects in ARS mice was due to altered H2R expression and/

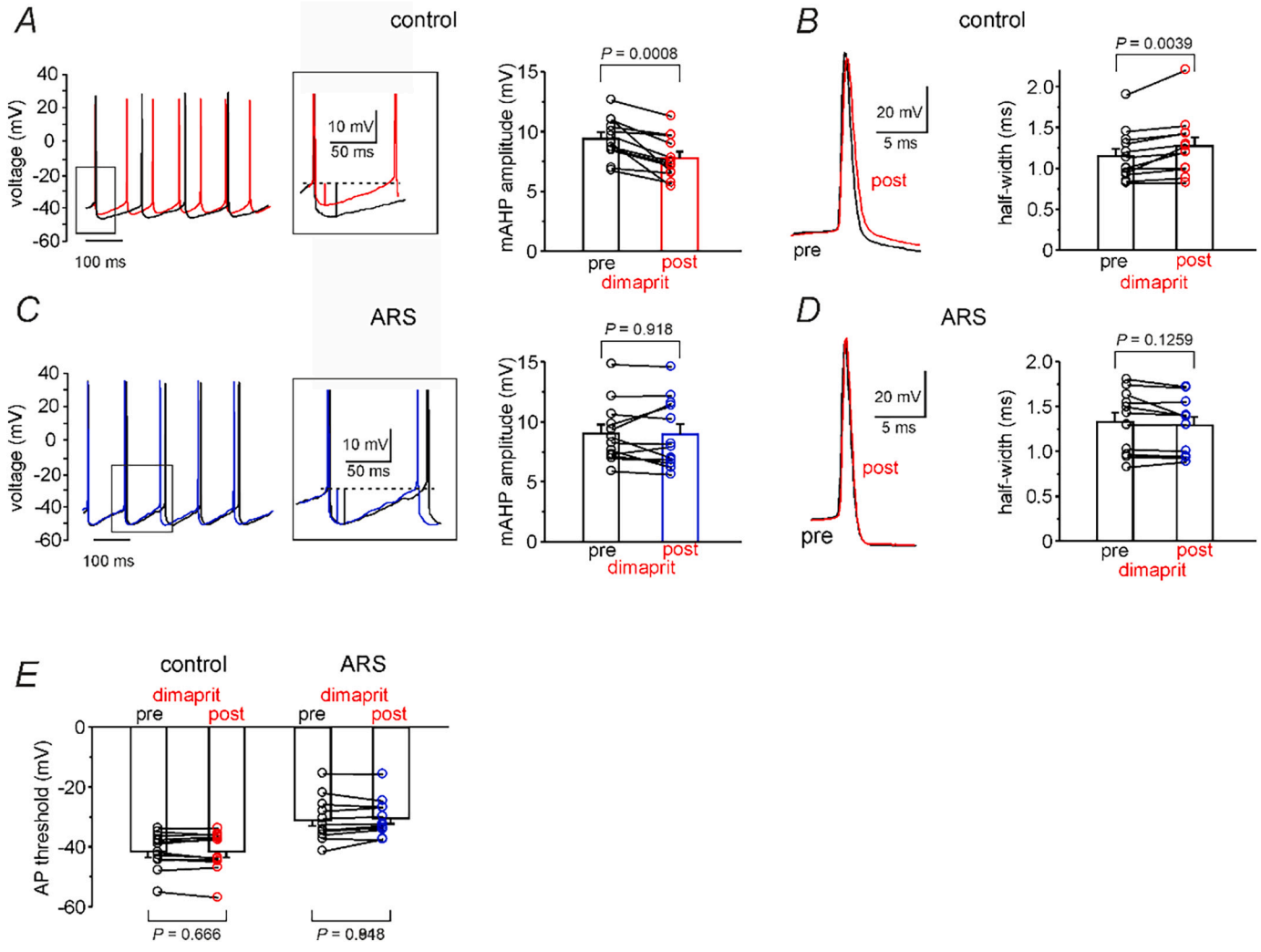

Fig. 2. mAHP amplitude and half-width are not modulated by H2R activation in MSNs from acute restraint mice.
(*A*) Left, representative traces showing reduced mAHP following dimaprit application in control mice. Right, bar graph depicting quantification of mAHP amplitude in the experimental conditions showed in panel *A* ($n = 12$ cells from 4 mice; p = 0.0008; paired Student's t-test). (*B*) Left, superimposition of APs highlighting decreased mAHP amplitude and broadened AP following dimaprit application in control mice. Right, summary plot showing mean values of AP half-width before and after dimaprit ($n = 12$ cells from 4 mice; p = 0.0039; paired Student's t-test). (*C* and *D*) Representative traces and bar graph showing that H2R activation did not affect mAHP and AP half-width in MSNs from ARS mice ($n = 12$ cells from 4 mice; p = 0.919 and 0.125 respectively; paired Student's t-test). (*E*) Summary plots illustrating that dimaprit perfusion had no effect on AP threshold in control and restraint mice ($n = 12$ cells from 4 mice; $p = 0.664$ and 0.151 respectively; paired Student's t-test).

or membrane distribution, we performed western blot analysis of NAc tissues from control and restraint mice. Tissues were lysed, separated into membrane and cytoplasmic fractions, and analyzed by western blotting. As shown in Supplementary Fig. 2B and C, the levels of H2R protein in the membrane and cytoplasmic fractions were not significantly different in the two groups, supporting our hypothesis that ARS recruits endogenous H2R signaling in NAc MSNs.

3.2. Acute restraint stress occludes the effect of H2R activation on Kv4.2 function

The downstream molecular mechanism responsible for the enhancement of evoked firing following H2R activation is due to PKA-dependent negative modulation of A-type potassium currents carried by Kv4.2 channels (Aceto et al., 2022). Accordingly, in control mice bath application of dimaprit elicited a decreased A-type K^+ current together with a significantly more depolarized activation voltage (Fig. 3 A and B; A-type K^+ current: pre = 2.28 ± 0.41 nA; post = 1.87 ± 0.29; n = 15 cells from 5 mice; p = 0.018; paired Student's t-test; $V_{1/2}$: pre = −12.7 ± 3.0 mV; post = −7.4 ± 3.0; n = 15 cells from 5 mice; p = 0.029; paired Student's t-test). As expected, when dimaprit was applied to MSNs obtained from ARS mice no changes in A-type K^+ current amplitudes and activation curves were detected (Fig. C; pre = 1.99 ± 0.38 nA; post = 1.74 ± 0.25 nA; n = 14 cells from 5 mice; p = 0.17; paired Student's t-test; $V_{1/2}$: pre = −16.1 ± 2.9 mV; post = −15.7 ± 2.9; n = 13 cells from 4 mice; p = 0.795; paired Student's t-test). Since H2R signaling activation, in addition to regulating Kv4.2 channel properties, induces the channel internalization in NAc MSNs (Aceto et al., 2022), we sought to determine whether the membrane distribution of Kv4.2 channels in NAc tissues from ARS mice was different compared to that evaluated in NAc tissues from control mice. Tissues were lysed, separated into membrane and cytoplasmic fractions, and analyzed by western blotting. As shown in Fig. 3 E and F, in ARS mice tissues the levels of Kv4.2 protein were decreased in the membrane fraction, whereas the cytoplasmic fraction of the protein was increased. These results indicate that membrane localization of Kv4.2 is decreased in the NAc of ARS exposed mice.

These results suggest that stress-evoked histamine release in the NAc occludes subsequent dimaprit-induced decrease in A-type K^+ currents.

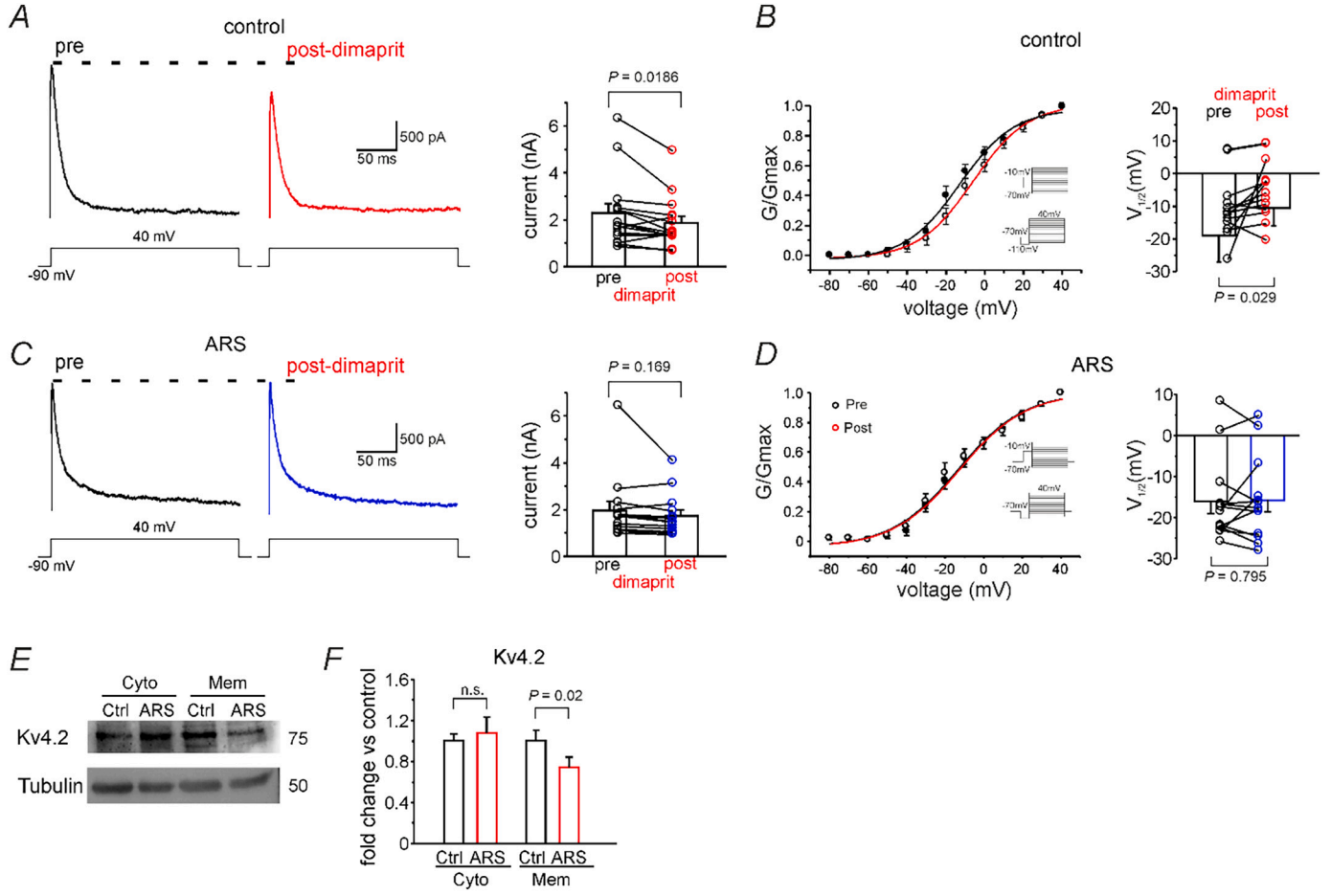

Fig. 3. Pharmacological activation of H2R failed to affect A-type K^+currents in mice exposed to acute restraint stress. (*A*) Left, representative traces showing transient A-type K^+ currents recorded in MSNs before (black) and after (red) dimaprit application in control mice. Right, summary plot showing the decreased A-type K^+ currents by dimaprit (n = 15 cells from 6 mice; p = 0.018; paired Student's t-test). (*B*) Left, activation curve showing the normalized A-type K^+ current conductance before and after dimaprit application in control mice. Note that the activation curve is shifted toward more depolarized membrane potential after dimaprit application. Right, bar graph showing mean ± SEM voltage at which ½ of the current was activated ($V_{1/2}$ acquired from a Bolzman fit of the curve). In control mice the mean V½ measured after dimaprit application was significantly different from that recorded before application (n = 15 cells from 6 mice; p = 0.029; paired Student's t-test), G, conductance; G_{max}, maximum G. (*C* and *D*) Representative traces and summary plots showing that H2R modulation of A-type K^+ currents was not observed in slices from ARS mice (A-type K^+ currents: n = 14 cells from 5 mice; p = 0.17; paired Student's t-test; V½: n = 13 cells from 4 mice; p = 0.799; paired Student's t-test). (*E*) Representative Western blots of NAc tissues showing Kv4.2 levels in membrane and cytosolic fractions from control and restraint mice. (*F*) Densitometry analysis for the blots probed with anti Kv4.2 channels and normalized to tubulin is shown. (N = 3 mice; statistics by ANOVA with Bonferroni post-hoc test; p = 0.02). (For interpretation of the references to colour in this figure legend, the reader is referred to the web version of this article.)

3.3. H2R antagonist treatment restores dimaprit's modulation of evoked firing and A-type K^+ currents in mice exposed to acute restraint stress

One explanation for all the findings reported so far is that stress-evoked H2R activity (ARS mice) occludes subsequent dimaprit-induced effects assessed ex vivo. If this hypothesis is correct, in vivo blockade of H2R during ARS exposure should protect dimaprit-induced modulation of intrinsic excitability and A-type K^+ currents.

Thus, 15 min prior to restraint stress, mice received an intraperitoneal injection of vehicle or the H2R antagonist zolantidine (10 mg/kg). Zolantidine was chosen over others H2R antagonists to its solubility profile, minimal collateral effects and because it can penetrate the blood-brain barrier (Laurino et al., 2015; Mohsen et al., 2014; Musilli et al., 2014; Naganuma et al., 2017). Since poor information are available on zolantidine's pharmacokinetic and because of the duration of ARS protocol (120 min) we decided to inject a second dose of zolantidine

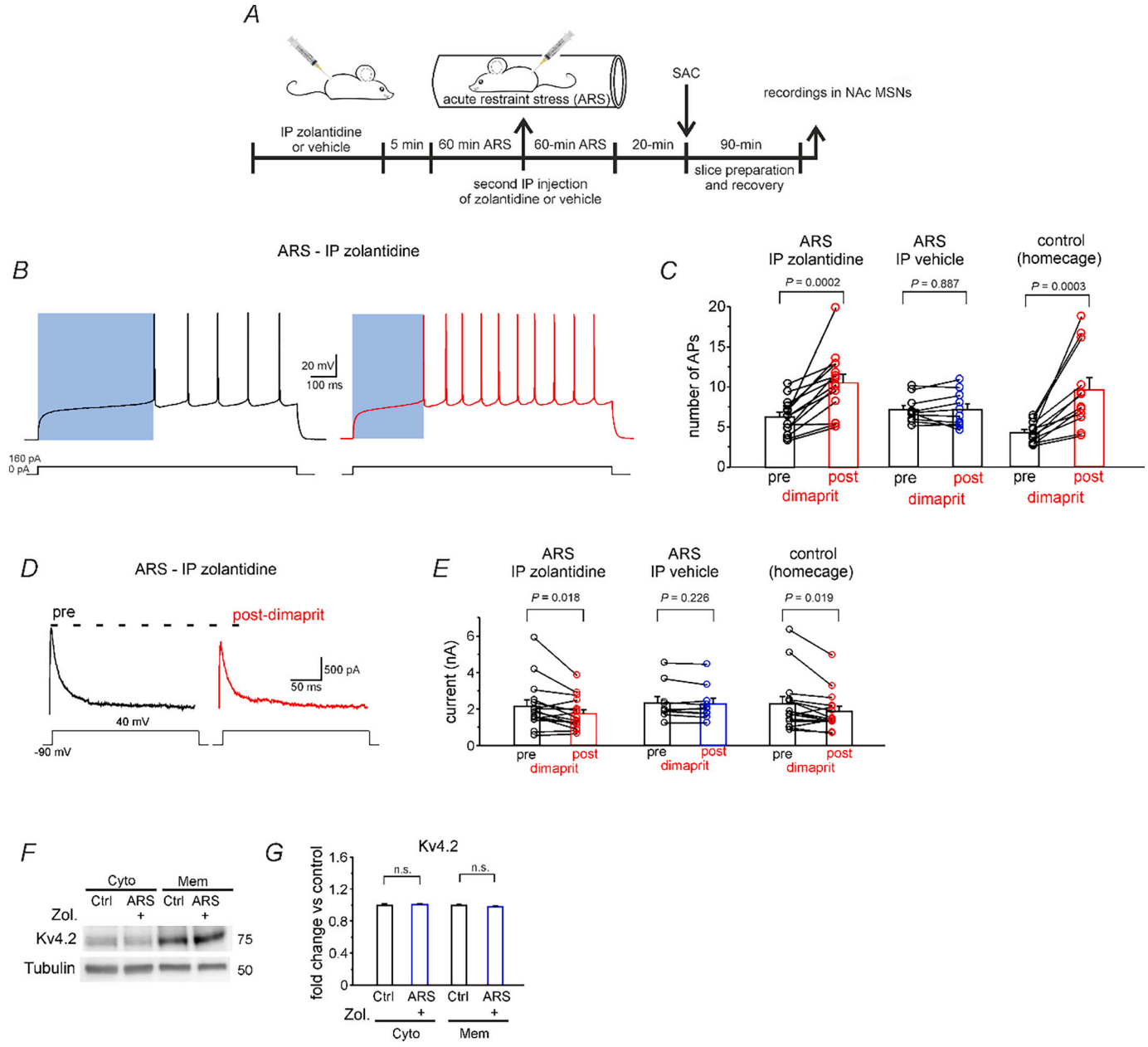

Fig. 4. H2R antagonist treatment in mice exposed to acute restraint stress restores dimaprit's modulation of evoked firing and A-type K^+currents. (A) Schematic depicting prophylactic treatment with H2R antagonist, zolantidine (Zol) prior and during restraint exposure. (*B*) Representative traces showing current-evoked firing of a MSN before and after local perfusion of dimaprit in zolantidine-treated mice exposed to ARS. (*C*) Bar graph depicting quantification of evoked firing in the experimental conditions showed in panel B ($n = 13$ cells from 4 mice; p = 0.0002; paired Student's *t*-test). For comparison, the effect of dimaprit on evoked firing in ARS mice injected with vehicle and control mice is also shown. Note that the increase in evoked firing in MSNs from zolantidine-treated ARS mice was comparable to that of control mice. (*D*) Representative traces showing transient A-type K^+ currents recorded in MSNs before and after dimaprit application in Zol-treated ARS mice. (E) Summary plot showing the decreased A-type K^+ currents by dimaprit ($n = 15$ cells from 6 mice; p = 0.018; paired Student's *t*-test). For comparison, dimaprit effect on A-type K^+ currents in ARS mice injected with vehicle (pre = 2.34 ± 0.33 nA; post = 2.27 ± 0.32; $n = 10$ cells from 4 mice; $p = 0.226$; paired Student's t-test) and control mice is also shown. (*F*) Representative western blot of NAc tissues showing Kv4.2 levels in membrane and cytosolic fractions from Zol-treated ARS exposed mice. (*G*) Densitometry analysis for the blots probed with anti Kv4.2 channels and normalized to tubulin is shown ($N = 3$ mice; statistics by ANOVA with Bonferroni post-hoc test; $p = 0.346$).

after 60 min of restraint stress to effectively blockade H2Rs during ARS (Fig. 4A). Administration of zolantidine in ARS mice restores the ability of dimaprit to affect both evoked firing (Fig. 4B and C; number of APs: pre = 6.35 ± 0.64; post = 10.88 ± 1.09; n = 13 cells from 5 mice; p = 0.0002; paired Student's t-test) and A-type K^+ currents (Fig. 4 D and E; pre = 1.97 ± 0.23 nA; post = 1.87 ± 0.29; n = 13 cells from 5 mice; p = 0.018; paired Student's t-test). Consistently, IP injection of zolantidine in ARS exposed mice restored dimaprit's effects on: *i*) the latency to fire, *ii*) the AHP amplitude, *iii*) the action potential half-width and *iv*) the activation curve of A-type K^+ currents (Supplementary Fig. 3 and Supplementary Table 1). Moreover, in ARS mice treated with zolantidine the levels of Kv4.2 protein were similar to what observed in control mice (Fig. 4 F and G).

Together, our findings indicate that ARS recruits endogenous H2R signaling in NAc MSNs and suggest a possible involvement of H2R/PKA/Kv4.2 axis in stress-induced behaviors.

3.4. H2R antagonist treatment ameliorates anxiety-like behavior in mice exposed to acute restraint stress

To determine whether altered H2R signaling contributed to ARS-induced anxiety-like behavior, we compared elevated plus maze (EPM)(Hogg, 1996) values in ARS mice receiving either vehicle (saline) or zolantidine. Of note, EPM test is routinely used to study anxiety-related behavior in mouse (Carola et al., 2002; Kraeuter et al., 2018).

As expected, mice injected with vehicle and exposed to the ARS protocol showed anxiety-like behavior (Fig. 5A). Indeed, in the EPM test, they spent significantly less time in the open arms and longer time in the closed arms compared to control mice injected with vehicle (Fig. 5B and C; EPM open arms: 14.2 ± 4.3 versus 37.5 ± 7.6 s; one-way ANOVA; $F_{(2,25)} = 8.72$; $p < 0.05$; followed by Tukey post hoc test; $p < 0.05$; EPM closed arm: 250.6 ± 7.4 versus 228.7 ± 6.6 s; one-way ANOVA; $F_{(2,25)} = 4.19$; $p < 0.05$; followed by Tukey post hoc test; $p < 0.05$; $n = 14$ and 11, respectively). Interestingly, when mice were injected with zolantidine and exposed to the ARS protocol, their behavioral phenotype was similar to that we observed in control mice and significantly different from restraint mice injected with vehicle, characterized by an anxiety-like phenotype (Fig. 5B and C; EPM open arm: 33.7 ± 5.7 versus 14.2 ± 4.3 s; one-way ANOVA; $F_{(2,25)} = 6.72$; $P < 0.05$; followed by Tukey post hoc test; *P < 0.05; EPM closed arm: 210.5 ± 14.9 versus 250.6 ± 7.4 s; oneway ANOVA; $F_{(2,25)} = 7.22$; $P < 0.05$; followed by Tukey post hoc test; **P < 0.05).

Because modulation of NAc circuitry affects anxiety and depression related behaviors (Wallace et al., 2009), our finding that zolantidine treatment in ARS mice prevents anxiety-like phenotype suggests that H2R signaling dysfunction serve as molecular mechanism of MSN maladaptive excitability underlying anxiety-like behaviors in ARS mouse model.

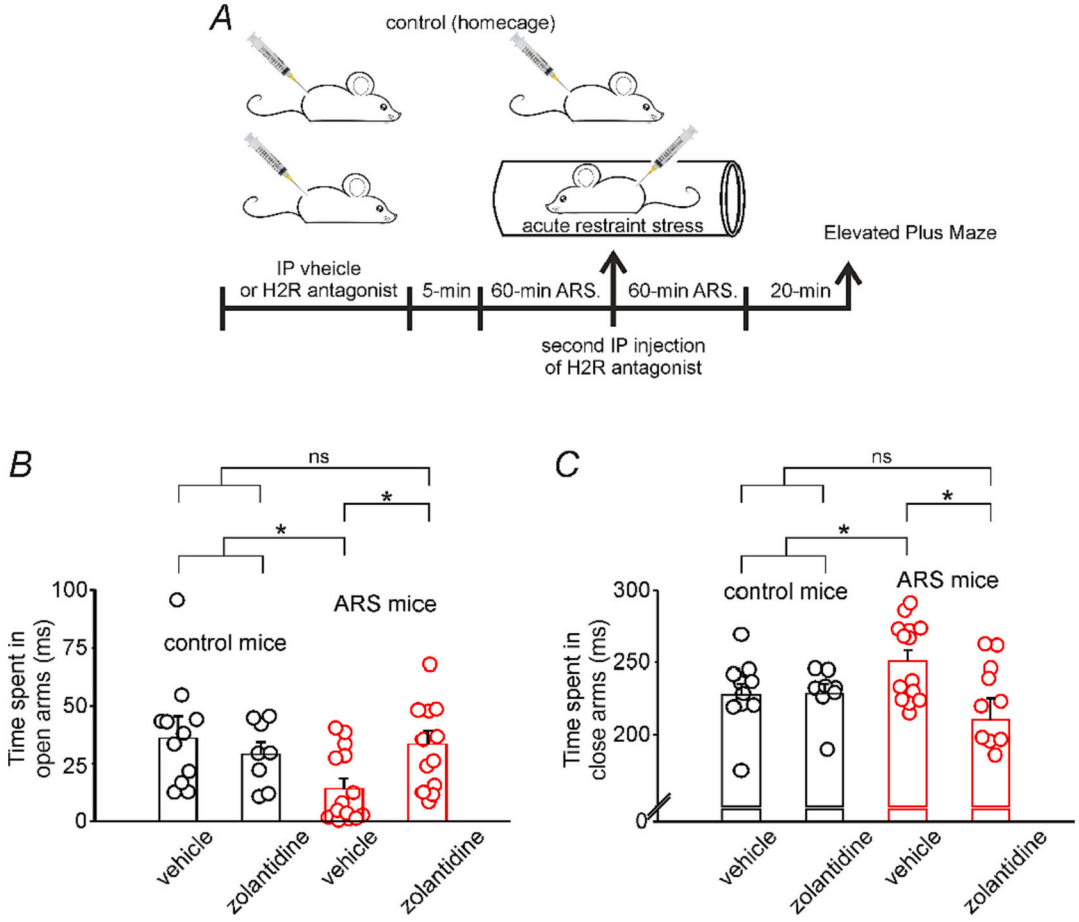

Fig. 5. Intraperitoneal injections of the H2R antagonist zolantidine ameliorates anxiety-like behavior in mice exposed to ARS protocol. (A) Experimental timeline. (B and C) Behavioral analysis by EPMs of ARS and control mice injected with either the vehicle or zolantidine. Of note, mice exposed to the ARS protocol and injected with vehicle showed anxiety-like phenotype compared with control mice injected with vehicle (one-way ANOVA; followed by Tukey post hoc test; $p >$ 0.05; n = 14 and 11, respectively). Noteworthy, the behavioral phenotype was significantly different in mice exposed to the ARS protocol and injected with zolantidine compared with mice exposed to the ARS protocol and injected with vehicle (one-way ANOVA; followed by Tukey post hoc test; $p > 0.05$). * $p < 0.05$; ** $p < 0.01$. ns, not significant. Error bars represent SEM, * $p < 0.05$, ** $p < 0.01$].

4. Discussion

The NAc has a pivotal role in the limbic basal ganglia loop, and its dysfunction results in psychiatric diseases including stress-related disorders such as anxiety and depression (Francis and Lobo, 2017; Gunaydin and Kreitzer, 2016). Indeed, accumulating experimental and clinical evidence indicates that the NAc holds a key position in motivation, emotion and cognition, and is strongly implicated in the treatment of stress-related disorders (Bagot et al., 2015; Christoffel et al., 2015). Previous studies have established the validity of the ARS paradigm as a reliable and robust model to investigate mechanisms underlying neuroadaptive changes, at the cellular and circuits levels, in response to stress (Buynitsky and Mostofsky, 2009). Here, we used ARS protocol to investigate neuroadaptive mechanisms in the NAc underlying anxiety-like behaviors, focusing on molecular mechanisms that could account for maladaptive intrinsic excitability of MSNs. In particular, we employed ARS paradigm as a means to recruit the TMN axis to assess whether endogenous histamine release activates H2R signaling in NAc MSNs. We found that histaminergic modulation of MSN excitability is missing following ARS exposure in H2R dependent manner. Much experimental evidence supports our conclusion: 1) pharmacological activation of H2R, by its selective agonist dimaprit, results in increased evoked firing and A-type K^+ current down-regulation in control mice but not in ARS exposed mice; 2) in vivo blockade of H2R, through intraperitoneal injection of the selective H2R antagonist zolantidine, restores dimaprit's effects; (3) ARS protocol increases histamine levels in the NAc while H2R expression and membrane localization are not affected; and (4) the ARS protocol decreases surface expression of Kv4.2 channels.

Our demonstration that H2R activation does not increase MSN excitability in mice exposed to ARS is based on our electrophysiological data showing that dimaprit application does not affect evoked firing and, nor the AP half width, mAHP and first spike latency which are modulated by H2R activation .

In our previous work we profiled the expression of H2R in MSNs of the NAc by using single-cell qRT-ddPCR (Aceto et al., 2022). We found that the vast majority of screened MSNs expressed H2R. Based on this finding and considering that H2R stimulation increased the excitability in the majority of recorded neurons, we speculated that activation of H2R enhances intrinsic excitability of both D1R and D2R MSNs. We confirmed this conclusion in the present study by showing that mRNA levels of H2R are comparable in both types of MSNs thus suggesting that ARS affects H2R signaling independently of MSN subtypes.

How does ARS exposure prevent H2R-dependent increase in MNS excitability?

It is well known that during behavioral states heightened awareness of salient environmental stimuli including acute stress and fear learning leads to enhanced output of histamine containing TMN neuron (Ito, 2000; Manz et al., 2021; Miklos and Kovacs, 2003; Taylor and Snyder, 1971). In our experimental condition, in line with this evidence, we found that ARS exposure increases histamine levels in NAc tissue (Supplementary Fig. 2A). It is conceivable that ARS exposure activated H2R signaling leading to saturation of the signaling pathway and, as consequence, occlusion of subsequent dimaprit–dependent effects on MSNs excitability assessed ex vivo in brain slices. Moreover, our data showing that in vivo blockade of H2R, by means of intraperitoneal injection of selective H2R antagonist zolantidine, restores the ability of H2R activation to increase MSN excitability in ARS exposed mice, strongly support our conclusion that ARS exposure recruits H2R signaling pathway. It should be considered that histaminergic afferents from the TMN are the most probable source of endogenous histamine in the NAc. However, histamine derived from mast cells cannot be excluded given that some studies indicate that acute stress triggered histamine degranulation (Baldwin, 2006; Theoharides et al., 1995). Nevertheless, the role of mast cell–derived histamine on MSN excitability remains to be elucidated.

Another possible explanation of the lack of dimaprit's effect on MSN excitability of ARS mice is an altered expression and/or membrane localization of H2R in these mice. However, our western blot experiments ruled out this possibility (Supplementary Fig. 2B and C).

We have recently demonstrated that Kv4.2 channels are the downstream targets of H2R signaling in NAc MSNs (Aceto et al., 2022). These channels underlay the rapidly activating and inactivating A-type K^+ current in MSNs of the NAc (Aceto et al., 2019). Operating at sub and suprathreshold voltages, Kv4.2 channels regulate AP repolarization and repetitive firing (Johnston et al., 2000). Moreover, it is well known that among the different channels contributing to AP kinetics, A-type K^+ channels contribute to AHP and AP duration (Kim et al., 2005; Storm, 1987; Zhang and McBain, 1995). Neurons with decreased A-type K^+ channel expression would have shorter AHP amplitudes and AP broadening, which are features allowing neurons to have higher AP firing frequency (Aceto et al., 2022; Carrasquillo et al., 2012; Kim et al., 2005). In our study all the H2R-dependent effects were found in MSNs of both control and zolantidine-treated ARS mice but not in vehicle-treated ARS mice. Additionally, our data showing that H2R activation failed to reduce A-type K^+ currents in MSNs of ARS mice, corroborate our conclusion that ARS exposure leads to saturation of the H2R signaling pathway. Of note, this conclusion is in line with a recent and elegant study showing that stress-evoked histamine release recruits a presynaptic gain control mechanism at glutamatergic synapse in the NAc, an effect that is mediated by H3R (Manz et al., 2021). In particular, this study showed that histamine negatively regulates glutamatergic transmission onto D1-MSNs via presynaptic H3R. This effect was substantially reduced following acute immobilization stress (AIS) in an NAc-specific, H3R-dependent manner given that pretreatment with an H3R antagonist intraperitoneally or microinfused into the NAc protects this plasticity. The author's interpretation for these findings was that AIS-evoked H3R activity occludes subsequent histamine-dependent modulation of excitatory synapse at D1-MSNs assessed ex vivo. Therefore, this study and our findings indicate that acute restraint stress recruits both H2R and H3R signaling in the NAc, thus affecting MSN excitability and glutamatergic synaptic transmission.

How our findings can be contextualized in the broad literature on stress-related neuropsychiatric disorders? The original monoamine theory postulates that the functionality of monoamines like serotonin, norepinephrine and dopamine is compromised during stress and depression (Belmaker and Agam, 2008; Harvey et al., 2004; Krystal and Neumeister, 2009). The more recent cytokine theory suggests that these impairments are downstream chemical effects of increased immune activity (pro-inflammatory cytokines) (Dantzer et al., 2008; Haase and Brown, 2015; Raison et al., 2006). Consistently, both pro-inflammatory cytokines and monoamines have been the target of partially effective pharmacological treatments (Bai et al., 2020). It has been recently suggested that stress-related brain disorders may be best explained by a hybrid of the monoamines and cytokine hypothesis in which histamine plays a fundamental role (Hersey et al., 2022). In the periphery, histamine is released from mast cells in response to stress or injury, allowing it to act as an immunomodulator (Schwartz et al., 1980). In the central nervous system (CNS), it is estimated that 50% of histamine originates from mast cells (Johnson and Krenger, 1992; Silver et al., 1996), but histamine can also be produced by neurons of the TMN in response to stress (Ito, 2000; Miklos and Kovacs, 2003; Panula and Nuutinen, 2013; Taylor and Snyder, 1971) and microglia (Katoh et al., 2001). Microglia can also be activated by histamine to produce proinflammatory cytokines (Dong et al., 2014). Such observations suggest that histamine is uniquely positioned to play a role in neuroinflammatory processes in the CNS and as such in the neuropathology observed in stress-related disorders. The spikes in brain histamine following stress likely drive neurochemical changes in monoaminergic systems that are believed to be dysregulated. For example, it has been shown that elevated histamine can result in increased activation of H3R that inhibits NE release (Schlicker et al., 1989), DA release (Schlicker et al., 1993) and 5HT release (Fink et al., 1990; Hashemi et al., 2011; Threlfell et al., 2004).

Therefore, it is likely that histamine may be a critical link between stress, monoamines, and cytokines in the initiation and progression of stress-related neuropsychiatric disorders.

Within this context, the ARS-dependent recruitment of H2R signaling we observed in the present study represents a novel mechanism by which elevated extracellular histamine levels regulate neuronal adaptation in brain areas involved in stress-dependent decisional strategies.

Our results also indicate that in vivo H2R blockade, by means of intraperitoneal administration of zolantidine, prevents ARS-induced anxiety phenotype (Fig. 5). Zolantidine is a potent selective H2R antagonist whose brain:blood ratio indicates that can penetrate the brain after peripheral administration (Calcutt et al., 1988). Moreover, a high concentration of zolantidine (100 mg/kg, s.c.) has no effect on whole brain levels of histamine, histamine metabolite tele-methylhistamine (t-MH), and brain histamine methyltransferase (HMT) activity, when measured 30 min after intraperitoneal administration in rats (Hough et al., 1988).

Early, studies have highlighted the potential of H2R antagonists to enhance the effects of opiate analgesics (Hasanein, 2011) and to exert a positive therapeutic effect on schizophrenia (Meskanen et al., 2013); hovewer, therapeutic applications for H2R antagonists in neuropsychiatric disorders are relatively rare to date. Our finding that zolantidine administration prevents ARS-induced anxiety phenotype suggests that activation of H2R contributes to the development of stress-related motivational states.

The contribution of different histamine receptors on modulatory control of emotional behaviors requires further studies. In this context, it is noteworthy that a recent study showed that the activation of the histaminergic afferent system inhibits glutamatergic synaptic transmission in the prelimbic prefrontal cortex to the NAc circuit by activating presynaptic H3R, and improves anxiety and obsessive-compulsive-like behaviors (OCD) induced by acute restraint stress (Zhang et al., 2020). Given the well-established role of the NAc in goal-directed behaviors, it is likely that H2R and H3R signaling contribute to anxiety-like behaviors in the acute restraint stress animal models.

Stress-related disorders, such as mood and anxiety disorders, show a pronounced gender bias in their age-of-onset, severity, prevalence (Altemus et al., 2014; Bangasser and Valentino, 2014; Brivio et al., 2018). It remains to be investigated whether ARS impairs H2R ability to modulate NAc MSN excitability also in female mice.

In conclusion, we describe here a novel molecular mechanism underlying vulnerability to anxiety and related intrinsic excitability in the NAc. Our results indicate that histamine in the NAc is recruited by the ARS protocol leading to engagement of H2R signaling. Our results also indicate that in vivo H2R blockade prevents ARS-induced anxiety behavior, thus suggesting that down-regulation of H2R signaling pathway may be a promising strategy for the management of stress-related motivational states.

Funding

This work was supported by Italian Ministry of University and Research (PRIN 2017-Prot. 2017K2NEF4 to MD) and Italian Ministry of Health, Ricerca Corrente – Fondazione Policlinico Universitario A. Gemelli IRCCS.

Author contributions

GA and LN designed, performed and analyzed electrophysiological experiments; CC, AB and LN performed Western blot experiments. GA and LN performed and analyzed behavioral experiments. GL and BT performed HPLC experiments. SN performed single-cell transcriptional analysis. MD and CG conceived the study supervised the work and wrote the paper. All authors gave approval to the final version of the manuscript.

Credit author statement

Conceptualization, M.D. and C.G.; Methodology, G.A. and L.N.; Data curation, G.A. and L.N; Investigation, G.A., L.N., S.N., A.B.; G.L; B.T; and C·C; Writing – Original Draft, M.D.; Writing – Review & Editing, M.D. and C.G.; Funding Acquisition, M.D.; Supervision, M.D.

Declaration of competing interest

All authors declare that the research was conducted in the absence of any commercial and financial relationships that could be construed as a potential conflict of interest.

Data availability

Data generated and/or analyzed during the current study will be made available from the corresponding author on request.

Acknowledgments

We would like to acknowledge the contribution of Electrophysiology Core Facilty G-STeP, of the Fondazione Policlinico Universitario “A. Gemelli” IRCCS for patch-clamp experiments.

Appendix A. Supplementary data

Supplementary data to this article can be found online at https://doi.org/10.1016/j.nbd.2022.105932.

References

Aceto, G., et al., 2019. GSK3β modulates timing-dependent long-term depression through direct phosphorylation of Kv4.2 channels. Cereb. Cortex 29, 1851–1865.
Aceto, G., et al., 2022. Activation of histamine type 2 receptors enhances intrinsic excitability of medium spiny neurons in the nucleus accumbens. J. Physiol. 600, 2225–2243.
Altemus, M., et al., 2014. Sex differences in anxiety and depression clinical perspectives. Front. Neuroendocrinol. 35, 320–330.
Amorini, A.M., et al., 2017. Severity of experimental traumatic brain injury modulates changes in concentrations of cerebral free amino acids. J. Cell. Mol. Med. 21, 530–542.
Arrigoni, E., Fuller, P.M., 2021. The Role of the Central Histaminergic System in Behavioral State Control. Curr Top Behav Neurosci.
Bagot, R.C., et al., 2015. Ventral hippocampal afferents to the nucleus accumbens regulate susceptibility to depression. Nat. Commun. 6, 7062.
Bai, S., et al., 2020. Efficacy and safety of anti-inflammatory agents for the treatment of major depressive disorder: a systematic review and meta-analysis of randomised controlled trials. J. Neurol. Neurosurg. Psychiatry 91, 21–32.
Baldwin, A.L., 2006. Mast cell activation by stress. Methods Mol. Biol. 315, 349–360.
Bangasser, D.A., Valentino, R.J., 2014. Sex differences in stress-related psychiatric disorders: neurobiological perspectives. Front. Neuroendocrinol. 35, 303–319.
Belmaker, R.H., Agam, G., 2008. Major depressive disorder. N. Engl. J. Med. 358, 55–68.
Bradford, M.M., 1976. A rapid and sensitive method for the quantitation of microgram quantities of protein utilizing the principle of protein-dye binding. Anal. Biochem. 72, 248–254.
Brivio, P., et al., 2018. TPH2 deficiency influences neuroplastic mechanisms and alters the response to an acute stress in a sex specific manner. Front. Mol. Neurosci. 11, 389.
Buynitsky, T., Mostofsky, D.I., 2009. Restraint stress in biobehavioral research: recent developments. Neurosci. Biobehav. Rev. 33, 1089–1098.
Cadwell, C.R., et al., 2016. Electrophysiological, transcriptomic and morphologic profiling of single neurons using patch-seq. Nat. Biotechnol. 34, 199–203.
Calcutt, C.R., et al., 1988. Zolantidine (SK&F 95282) is a potent selective brain-penetrating histamine H2-receptor antagonist. Br. J. Pharmacol. 93, 69–78.
Carola, V., et al., 2002. Evaluation of the elevated plus-maze and open-field tests for the assessment of anxiety-related behaviour in inbred mice. Behav. Brain Res. 134, 49–57.
Carrasquillo, Y., et al., 2012. A-type K+ channels encoded by Kv4.2, Kv4.3 and Kv1.4 differentially regulate intrinsic excitability of cortical pyramidal neurons. J. Physiol. 590, 3877–3890.
Christoffel, D.J., et al., 2015. Excitatory transmission at thalamo-striatal synapses mediates susceptibility to social stress. Nat. Neurosci. 18, 962–964.
Dantzer, R., et al., 2008. From inflammation to sickness and depression: when the immune system subjugates the brain. Nat. Rev. Neurosci. 9, 46–56.
D'Ascenzo, M., et al., 2009. Activation of mGluR5 induces spike afterdepolarization and enhanced excitability in medium spiny neurons of the nucleus accumbens by modulating persistent Na+ currents. J. Physiol. 587, 3233–3250.

Dong, H., et al., 2014. Histamine induces upregulated expression of histamine receptors and increases release of inflammatory mediators from microglia. Mol. Neurobiol. 49, 1487–1500.
Duman, R.S., et al., 2016. Synaptic plasticity and depression: new insights from stress and rapid-acting antidepressants. Nat. Med. 22, 238–249.
Fink, K., et al., 1990. Involvement of presynaptic H3 receptors in the inhibitory effect of histamine on serotonin release in the rat brain cortex. Naunyn Schmiedeberg's Arch. Pharmacol. 342, 513–519.
Francis, T.C., Lobo, M.K., 2017. Emerging role for nucleus accumbens medium spiny neuron subtypes in depression. Biol. Psychiatry 81, 645–653.
Gunaydin, L.A., Kreitzer, A.C., 2016. Cortico-basal ganglia circuit function in psychiatric disease. Annu. Rev. Physiol. 78, 327–350.
Haase, J., Brown, E., 2015. Integrating the monoamine, neurotrophin and cytokine hypotheses of depression–a central role for the serotonin transporter? Pharmacol. Ther. 147, 1–11.
Harvey, B.H., et al., 2004. Serotonin and stress: protective or malevolent actions in the biobehavioral response to repeated trauma? Ann. N. Y. Acad. Sci. 1032, 267–272.
Hasanein, P., 2011. Effects of histamine H3 receptors on chemical hyperalgesia in diabetic rats. Neuropharmacology. 60, 886–891.
Hashemi, P., et al., 2011. In vivo electrochemical evidence for simultaneous 5-HT and histamine release in the rat substantia nigra pars reticulata following medial forebrain bundle stimulation. J. Neurochem. 118, 749–759.
Hersey, M., et al., 2022. Integrating the monoamine and cytokine hypotheses of depression: is histamine the missing link? Eur. J. Neurosci. 55, 2895–2911.
Hogg, S., 1996. A review of the validity and variability of the elevated plus-maze as an animal model of anxiety. Pharmacol. Biochem. Behav. 54, 21–30.
Hough, L.B., et al., 1988. Actions of the brain-penetrating H2-antagonist zolantidine on histamine dynamics and metabolism in rat brain. Biochem. Pharmacol. 37, 4707–4711.
Ito, C., 2000. The role of brain histamine in acute and chronic stresses. Biomed. Pharmacother. 54, 263–267.
Johnson, D., Krenger, W., 1992. Interactions of mast cells with the nervous system–recent advances. Neurochem. Res. 17, 939–951.
Johnston, D., et al., 2000. Dendritic potassium channels in hippocampal pyramidal neurons. J. Physiol. 525 (Pt 1), 75–81.
Katoh, Y., et al., 2001. Histamine production by cultured microglial cells of the mouse. Neurosci. Lett. 305, 181–184.
Kim, J., et al., 2005. Kv4 potassium channel subunits control action potential repolarization and frequency-dependent broadening in rat hippocampal CA1 pyramidal neurones. J. Physiol. 569, 41–57.
Kraeuter, A.K., et al., 2018. Neuropsychiatric sequelae of early nutritional modifications: a beginner's guide to behavioral analysis. Methods Mol. Biol. 1735, 403–420.
Krystal, J.H., Neumeister, A., 2009. Noradrenergic and serotonergic mechanisms in the neurobiology of posttraumatic stress disorder and resilience. Brain Res. 1293, 13–23.
Kupchik, Y.M., et al., 2015. Coding the direct/indirect pathways by D1 and D2 receptors is not valid for accumbens projections. Nat. Neurosci. 18, 1230–1232.
Laurino, A., et al., 2015. In the brain of mice, 3-iodothyronamine (T1AM) is converted into 3-iodothyroacetic acid (TA1) and it is included within the signaling network connecting thyroid hormone metabolites with histamine. Eur. J. Pharmacol. 761, 130–134.
Lazzarino, G., et al., 2020. Low molecular weight dextran sulfate (ILB((R))) administration restores brain energy metabolism following severe traumatic brain injury in the rat. Antioxidants (Basel). 9.
Lister, R.G., 1987. The use of a plus-maze to measure anxiety in the mouse. Psychopharmacology 92, 180–185.
Manz, K.M., et al., 2021. Histamine H3 receptor function biases excitatory gain in the nucleus accumbens. Biol. Psychiatry 89, 588–599.
Mazurkiewicz-Kwilecki, I.M., Prell, G.D., 1986. Brain histamine response to stress in 12 month old rats. Life Sci. 38, 2339–2345.
McEwen, B.S., et al., 2015. Mechanisms of stress in the brain. Nat. Neurosci. 18, 1353–1363.
Meskanen, K., et al., 2013. A randomized clinical trial of histamine 2 receptor antagonism in treatment-resistant schizophrenia. J. Clin. Psychopharmacol. 33, 472–478.
Miklos, I.H., Kovacs, K.J., 2003. Functional heterogeneity of the responses of histaminergic neuron subpopulations to various stress challenges. Eur. J. Neurosci. 18, 3069–3079.
Mohsen, A., et al., 2014. Mechanism of the histamine H(3) receptor-mediated increase in exploratory locomotor activity and anxiety-like behaviours in mice. Neuropharmacology. 81, 188–194.
Musilli, C., et al., 2014. Histamine mediates behavioural and metabolic effects of 3-iodothyroacetic acid, an endogenous end product of thyroid hormone metabolism. Br. J. Pharmacol. 171, 3476–3484.
Naganuma, F., et al., 2017. Histamine N-methyltransferase regulates aggression and the sleep-wake cycle. Sci. Rep. 7, 15899.
Nestler, E.J., Carlezon Jr., W.A., 2006. The mesolimbic dopamine reward circuit in depression. Biol. Psychiatry 59, 1151–1159.
Nomura, H., et al., 2019. Central histamine boosts Perirhinal cortex activity and restores forgotten object memories. Biol. Psychiatry 86, 230–239.
Panula, P., Nuutinen, S., 2013. The histaminergic network in the brain: basic organization and role in disease. Nat. Rev. Neurosci. 14, 472–487.
Pitman, R.K., et al., 2012. Biological studies of post-traumatic stress disorder. Nat. Rev. Neurosci. 13, 769–787.
Possieri, C., et al., 2021. Combined molecular and mathematical analysis of long noncoding RNAs expression in fine needle aspiration biopsies as novel tool for early diagnosis of thyroid cancer. Endocrine. 72, 711–720.
Provensi, G., et al., 2020. Brain histamine modulates recognition memory: possible implications in major cognitive disorders. Br. J. Pharmacol. 177, 539–556.
Raison, C.L., et al., 2006. Cytokines sing the blues: inflammation and the pathogenesis of depression. Trends Immunol. 27, 24–31.
Sadler, A.M., Bailey, S.J., 2016. Repeated daily restraint stress induces adaptive behavioural changes in both adult and juvenile mice. Physiol. Behav. 167, 313–323.
Schlicker, E., et al., 1989. Inhibition of noradrenaline release in the rat brain cortex via presynaptic H3 receptors. Naunyn Schmiedeberg's Arch. Pharmacol. 340, 633–638.
Schlicker, E., et al., 1993. Histamine inhibits dopamine release in the mouse striatum via presynaptic H3 receptors. J. Neural Transm. Gen. Sect. 93, 1–10.
Schwartz, A., et al., 1980. Histamine inhibition of the in vitro induction of cytotoxic T-cell responses. Immunopharmacology. 2, 179–190.
Silver, R., et al., 1996. Mast cells in the brain: evidence and functional significance. Trends Neurosci. 19, 25–31.
Storm, J.F., 1987. Action potential repolarization and a fast after-hyperpolarization in rat hippocampal pyramidal cells. J. Physiol. 385, 733–759.
Taylor, K.M., Snyder, S.H., 1971. Brain histamine: rapid apparent turnover altered by restraint and cold stress. Science. 172, 1037–1039.
Theoharides, T.C., et al., 1995. Stress-induced intracranial mast cell degranulation: a corticotropin-releasing hormone-mediated effect. Endocrinology. 136, 5745–5750.
Threlfell, S., et al., 2004. Histamine H3 receptors inhibit serotonin release in substantia nigra pars reticulata. J. Neurosci. 24, 8704–8710.
Venner, A., et al., 2019. Reassessing the role of histaminergic tuberomammillary neurons in arousal control. J. Neurosci. 39, 8929–8939.
Wallace, D.L., et al., 2009. CREB regulation of nucleus accumbens excitability mediates social isolation-induced behavioral deficits. Nat. Neurosci. 12, 200–209.
Yoshikawa, T., et al., 2021. Histaminergic neurons in the tuberomammillary nucleus as a control Centre for wakefulness. Br. J. Pharmacol. 178, 750–769.
Zhang, L., McBain, C.J., 1995. Potassium conductances underlying repolarization and after-hyperpolarization in rat CA1 hippocampal interneurones. J. Physiol. 488 (Pt 3), 661–672.
Zhang, X.Y., et al., 2020. Targeting presynaptic H3 heteroreceptor in nucleus accumbens to improve anxiety and obsessive-compulsive-like behaviors. Proc. Natl. Acad. Sci. U. S. A. 117, 32155–32164.
Zhuang, Q.X., et al., 2018. Histamine excites striatal dopamine D1 and D2 receptor-expressing neurons via postsynaptic H1 and H2 receptors. Mol. Neurobiol. 55, 8059–8070.